Article

Affinity Binding-Induced Hg2+ Releasing and Quantum Dot Doping for General, Label-Free, and Homogenous Fluorescence Protein Assay

Yishen Tian, Chen Xin, Shuang Liu, Ying Liu, and Shufeng Liu

ACS Sens., **Just Accepted Manuscript** • DOI: 10.1021/acssensors.8b00316 • Publication Date (Web): 15 Jun 2018

Affinity Binding-induced Hg^{2+} releasing and Quantum Dot Doping for General, Label-Free, and Homogenous Fluorescence Protein Assay

Yishen Tian, Chen Xin, Shuang Liu, Ying Liu, and Shufeng Liu*

Key Laboratory of Sensor Analysis of Tumor Marker, Ministry of Education, College of Chemistry and Molecular Engineering, Qingdao University of Science and Technology, No. 53, Rd. Zhengzhou, Qingdao, Shandong 266042, China.

*Corresponding author. Tel. & Fax. 86-532-84022681. E-mail address: sliu@qust.edu.cn

Abstract

Herein, a general protein conversion and analysis strategy was well developed for homogenous, label-free, and sensitive protein detection, which was on the basis of the affinity binding-induced Hg^{2+} releasing for protein conversion, and the succeeding Hg^{2+} doping-induced ZnSe quantum dot (QD) photoluminescence for signal readout. Two DNA motifs were designed, and each of which was conjugated with a protein-specific recognition ligand. The mercury ions were initially introduced into one DNA motif by T-Hg^{2+}-T interaction. The Hg^{2+} releasing was then accomplished after protein recognition-initiated strand exchange reaction between two DNA motifs. Then, the simultaneous incorporation of the released Hg^{2+} into ZnSe QD resulted in a doping-dependent fluorescence emission at 560 nm correlated with protein analysis. The protein assay is outperformed only by a simple one-step mixing operation but no any separation or washing steps. Also, the use of doped QD as a fluorogenic reporter can avoid the fluorophore and/or quencher labeling, and eliminate complex DNA manipulation procedures for signal readout or amplification involved in the existing most nucleic acid-based protein conversion and analysis methods. The versatile and sensitive detection toward multivalent proteins was verified with the detection limits achieved as 0.034 nM for anti-Dig antibody, 0.012 nM for streptavidin and 0.025 nM for thrombin. Thus, it shows a great promise for protein analysis to accommodate the applications in disease diagnosis, biomarker screening, and clinical medicine.

Keywords: Protein biosensor; Affinity binding; DNA strand displacement reaction, Quantum dot doping; Mercury ion

Specific protein detection is of significant importance for disease diagnosis and monitoring, clinical medicine and prognosis evaluation.[1-4] The commonly employed protein analysis techniques including sandwich enzyme-linked immunosorbent assays (ELISA) and western blotting are often involved with several reagent- or wash-intensive operation processes, dedicated instrumentation and specialized technicians.[5-7] Also, these assay formats are relatively inflexible to apply to other targets. These constraints impede their popularity into the resource-constrained regions to some extent, easily resulting in a delay for disease diagnosis and clinical treatment. Therefore, the development of flexible, easy-to-operate, highly sensitive and selective protein detection technologies is imperative to accommodate the rapid progress in clinical diagnostics, biomarkers screening, and understanding of biological and physiological functions of clinically relevant biomolecules.

Over the past years, the design of nucleic acid-based protein conversion and detection strategies has attracted substantial attention, owing to the exquisite specificity of base pairing, cost-effective, ease of modification, resistance to denaturation, and remarkable structure features of nucleic acid.[8-12] By virtue of protein conversion strategies, the protein recognition event could be quantitatively conveyed into specific DNA output or other easy-to-detect information. For example, a terminal DNA protection assay with the aid of specific nucleases has been well proposed to convey protein binding event into reserved DNA fragment for further analysis.[13-15] But the use of specific nuclease to validate protein binding is essential. The recently proposed affinity binding-induced DNA annealing or assembly could be regarded as another typical protein conversion strategy. The target protein recognition with two separate affinity probes creates an opportunity to enhance the stability of DNA duplexes for DNA annealing or assembly.[16-20] The further manipulation of output DNA is responsible for signal readout or amplification, reflecting protein quantification.[21-26] These and other nucleic acid-based protein conversion strategies have shown a set of attractive

features, for example homogenous operation with no need for separation, flexibility for different targets, and easy adaptation to multiple detection or amplification means.[27-32] However, the required additional operation toward the DNA output for signal readout or simplification might be easily confronted with the increased assay complexity and reduced analysis accuracy. Also, in most cases of fluorescence signal readout, the necessary fluorophore and/or quencher labeling on the introduced DNA reporter likely suffers from undesirable background and increased cost. Therefore, the development of facile and direct signal readout after protein conversion, eliminating subsequent complex nucleic acid operation procedures and labeling of signal molecules, would be much sought-after. Inspired by the interaction of metal ions with nucleobases,[33-36] and the metal ion-doped quantum dot (QD) photoluminescence,[37-39] the design of suitable protein conversion strategy to convey the protein recognition into the specific metal ion, followed by metal ion-doped QD photoluminescence, is envisioned to offer a promising avenue for protein biosensing.

Herein, a proof-of-principle study for versatile, label-free, sensitive, selective and homogenous protein biosensing was conducted, which combined protein recognition-initiated DNA strand exchange reaction for Hg^{2+} releasing and subsequent QD doping for fluorescence generation. Protein could be simultaneously recognized by two affinity ligands that were conjugated to two respective DNA motifs. The mercury ions were initially introduced into one DNA motif based on T-Hg^{2+}-T interaction. Then, the protein binding with two affinity probes increased the local concentration of these two DNA motifs to accelerate the strand displacement reaction between them.[40,41] As a consequence, the Hg^{2+} was released and then spontaneously incorporated into the ZnSe QD, inducing a doping-dependent fluorescence emission for protein quantification. QD has been largely explored for biosensing and bioimaging applications since its facile synthesis, relatively good stability, robust optical performance, and low toxicity.[42-45] Herein, the employment of protein recognition-initiated DNA strand exchange reaction is

committed to liberate Hg^{2+}, regardless of output DNA or assembly. The further Hg^{2+} doping of QD to induce photoluminescence is directly used as a fluorogenic reporter. Thus, it affords a new and well-controlled manner for protein analysis. The detection generality of the proposed strategy toward different proteins could be readily achieved by replacing the affinity ligands conjugated on the motif DNA.

Experimental section

Materials and chemicals. Sheep polyclonal anti-digoxigenin (anti-Dig) antibody, thrombin from human plasma (lyophilized powder, ≥2,000 NIH units/mg protein), mouse immunoglobin G (IgG), L-glutathione (GSH, ≥98%), selenium powder (99.99%), sodium borohydride (≥98%) and zinc acetate dihydrate (≥99.0%) were obtained from Sigma-Aldrich (St. Louis, MO, USA). Streptavidin, bovine serum albumin (BSA), and α-fetoprotein (AFP) were received from Beijing Dingguo Biotech Co., Ltd. (Beijing, China). Mercury (II) perchlorate trihydrate (≥99.0%) was bought from Strem Chemicals, Inc. (France). Acrylamide/bisacrylamide gel solution, ammonium persulfate (APS), ethidium bromide (EB), and N,N,N′,N′-tetramethylethylenediamine (TEMED) were obtained from Yantai Science and Biotechnology Co., Ltd. (Yantai, China). Fetal calf serum and synthesized HPLC-purified oligonucleotide sequences (shown in Table S1) were obtained from Sangon Biotech. Co., Ltd. (Shanghai, China). Other chemicals were of analytical grade, and purchased from Shanghai Chemical Reagents (Shanghai, China).

Synthesis of ZnSe QD. ZnSe QD was synthesized according to the reported procedure.[45] Briefly, 1 mL of 250 mM NaHSe solution was firstly obtained after reaction of selenium powder (0.0197 g) with the freshly prepared sodium borohydride (0.02 g) at room temperature. Then, the zinc acetate (125 μL, 100 mM) was mixed with GSH (93.75 μL, 200 mM), and diluted with 0.2 M NH_4HCO_3 solution (pH 12.3) to 500 μL. Followed by rapid injection of NaHSe solution (25 μL, 250 mM) into the above mixed solution and vortex oscillation for 10 s, the ZnSe QD was obtained. After centrifugal purification for 10 min

via a 3K centrifugal device (Pall Corporation) at 13500 rpm, the ZnSe QD was collected and diluted to the original volume by using 0.2 M NH_4HCO_3 solution.

Protein detection. The detection procedure for anti-Dig antibody was listed as below. A stock solution of duplex AB probe was firstly prepared by mixing 20 μL of 2 μM motif A strand, 20 μL of 2 μM blocking strand B, and 40 μL of 2 μM Hg^{2+} into 120 μL of 0.05 M Tris buffer (pH 7.5) at 37 °C for 60 min. Then, 10 μL of 200 nM obtained duplex AB probe, 10 μL of 200 nM motif C strand and varying concentrations of anti-Dig antibody (10 μL) were added into 160 μL of 0.05 M Tris buffer (pH 7.5) and incubated for 60 min at 37 °C. After that, 10 μL of ZnSe QD solution was added for fluorescence response. The above operation procedures were also suitable for streptavidin and thrombin detection.

Polyacrylamide gel electrophoresis. A 17.5% polyacrylamide hydrogel was firstly prepared by adding 40% gel solution (39:1, 3.5 mL), 50×TAE Buffer (160 μL), 10% APS (80 μL) and TEMED (4 μL) into 4256 μL water. Then, the polyacrylamide gel electrophoresis (PAGE) experiments were operated at room temperature in 1×TAE buffer with the applied voltage of 180 V for 3 min and 135 V for 90 min. After that, the gels were stained with EB dye.

Instruments. The fluorescence spectroscopy was recorded with a F-2700 spectrometer. The scan rate, excitation wavelength, 24 photomultiplier voltage, and slits of excitation and emission were set at 1500 nm/min, 320 nm, 700 V, and 5 nm/5 nm, respectively. The morphology characterization was conducted by a JEM-2100F transmission electron microscope (JEOL, 200 kV). X-Ray photoelectron spectroscopy (XPS) was characterized by using a Thermo scientific ESCALAB 250Xi spectrometer with Al Ka excitation (1486 eV). A FR-980 gel imager (Shanghai, China) was used to capture the gel images.

RESULTS AND DISCUSSIONS

Design principle of affinity binding-induced Hg^{2+} releasing for protein

biosensing. Herein, the protein biosensor was fabricated based on the affinity binding-induced Hg^{2+} releasing for protein conversion, and the succeeding Hg^{2+} doping-induced ZnSe QD photoluminescence for signal readout. The anti-digoxin (anti-Dig) antibody was firstly chosen as a model protein and its biosensing principle was schematically shown in Scheme 1. The DNA motifs (A and C) were designed, which were conjugated with the affinity ligand (herein Dig) at 5′ and 3′-terminus, respectively, for protein recognition. The DNA motif A contains the complementary base sequences at 3′-terminus with the blocking strand B except two T-T mismatches. The incorporation of Hg^{2+} into the hybrids between the motif A and the blocking strand B by T-Hg^{2+}-T interaction could enhance duplex stability. It can also inhibit the undesirable target-independent DNA assembly between two DNA motifs (A and C), which contains mutual base complementarities (12 bases). After protein recognition with the conjugated ligands, the DNA motifs (A and C) are brought proximity with the increased local concentrations to accelerate the strand exchange between duplex AB and strand C.[40,41] This induces the releasing of blocking strand B from motif A, accompanied with the Hg^{2+} releasing. Subsequently, the ZnSe QD in the solution could be spontaneously incorporated by the released Hg^{2+}, giving rise to a doping-dependent fluorescence emission for protein quantification. However, in case of no protein target, the strand displacement between AB duplex and strand C could not autonomously occur for Hg^{2+} releasing. The sequestered Hg^{2+} in the DNA duplex AB would be not accessible for QD doping. By adopting different types of affinity ligands conjugated to the DNA motifs, such detection principle should be readily applied for various protein targets. The detection toward streptavidin and thrombin would be discussed later in this study. Thus, the current study that makes full use of affinity binding-induced Hg^{2+} releasing and doping-dependent QD photoluminescence would provide a good choice for versatile, label-free, sensitive, selective and in-solution protein detection.

<<Herein Scheme 1>>

Hg^{2+} doping-induced ZnSe QD photoluminescence. The synthesized ZnSe QD was characterized by TEM with a near-spherical morphology and an average size of around 3.3 nm (Figure 1A and Figure S1). Figure 1B shows the XPS spectra of ZnSe QD before and after Hg^{2+} doping. The peaks for Se 3d, Zn 2p, C 1s at specific positions could be seen in the spectrum of the initial ZnSe QD. After its incubation with Hg^{2+}, in addition to the characteristic peaks of ZnSe QD, peaks for Hg 4f were clearly observed, indicating the successful incorporation of Hg^{2+} into ZnSe QD. To verify Hg^{2+} doping-induced ZnSe QD photoluminescence, the Hg^{2+} with various concentrations were added respectively into the ZnSe QD solution and the photoluminescence spectra were immediately recorded. It could be seen from Figure 1C, a new emission peak at 560 nm could be generated after Hg^{2+} doping of ZnSe QD and its intensity increased gradually with an increasing amount of Hg^{2+}, ranging from 0 to 50 nM. Such an emission peak at 560 nm could not be observed in case of no Hg^{2+}. Also, this emission response at 560 nm is only specific to the added Hg^{2+} at the tested metal ions (Figure S2). The calibration relationship between the fluorescence intensity of the doped ZnSe QD at 560 nm and the Hg^{2+} concentration was plotted in Figure 1D. The doped QD showed an especially pronounced responsivity to Hg^{2+} at a concentration range of 0-10 nM. The Hg^{2+} concentration even at 0.5 nM could be well discriminated by current QD doping method, indicating its application possibility for direct and sensitive Hg^{2+} analysis. Although the doping and responsive mechanism of QD was still underexploited at this time, it could be adopted as a superior signal generator to explore its applications in metal ion and metal ion-related target analysis.

<<Herein Figure 1>>

Detection feasibility toward anti-Dig antibody. The melting temperatures of the AB duplex after introduction or not of Hg^{2+} were measured as 52 and 37 °C, respectively, indicating the specific incorporation of Hg^{2+} into T-T base pair for the enhanced stability of duplex AB (Figure 2A). To verify protein recognition-initiated strand exchange for the concomitant Hg^{2+} releasing and

its further doping-induced QD photoluminescence, the corresponding fluorescence experiments were conducted (Figure 2B). The initial ZnSe QD showed only an emission peak at around 405 nm (black line), which was disappeared and a new emission peak arose at 560 nm after Hg^{2+} doping (green line). Upon incubation of anti-Dig antibody with the mixture of affinity probe (AB duplex and motif C), a distinct emission peak at 560 nm but no emission peak at 405 nm could be also observed (blue line), which was almost the same behavior as the doped ZnSe QD, differing only by a decreased intensity. This strongly indicated that the Hg^{2+} was successfully released from the original duplex AB and available for QD doping after affinity recognition-initiated strand exchange process. The control experiment in the absence of anti-Dig antibody revealed only a weak decrease of emission peak at 405 nm of QD but no new emission peak at 560 nm (red line), indicating that the Hg^{2+} specifically incorporated into the T-T base pair of duplex AB was not available for QD doping. We also made a comparative study by using the DNA motifs with only one (A or C) conjugated by the Dig recognition element. No emission responses at 560 nm could be identified in these cases (Figure S3), verifying that the Hg^{2+} releasing was definitely ascribed to the affinity recognition of protein with its two ligands for the succeeding intramolecular strand exchange reaction between duplex AB and motif C. The protein recognition-initiated DNA strand exchange process was also evidenced by PAGE experiments (Figure 2C). Lane 3 and 4 shows the bands for the motif C and duplex AB, respectively. In the case of no anti-Dig antibody, the bands corresponding to the duplex AB and motif C could be only seen (lane 2), indicating that strand exchange rate between duplex AB and motif C was very sluggish. Upon addition of anti-Dig antibody, two new bands were observed (lane 1). The upper band with a very slow migration rate could be ascribed to the new generated complex by the anti-Dig antibody and the hybrids of motif A and C. The lower band with a relatively rapid migration rate was related to the new released strand B after protein recognition-initiated DNA strand exchange process. The PAGE experiments

also evidenced the affinity recognition-initiated DNA strand exchange between duplex AB and motif C for strand B and Hg^{2+} releasing. The protein recognition-initiated strand exchange process for Hg^{2+} releasing was also dynamically monitored. The fluorescence intensity of doped QD increased stepwise with the extended protein incubation time and a plateau value could be almost reached at 60 min (Figure 2D). Thus, the proposed strategy for protein detection could be achieved within 60 min.

<<Herein Figure 2>>

Sensing performance of the proposed strategy toward anti-Dig antibody. The sensing performance of the developed protein biosensor was then conducted by titrating different dosages of anti-Dig antibody (0-20 nM) against the sensing system containing 10 nM AB duplex and 10 nM strand C (Figure 3A). The fluorescence intensities of doped QD at 560 nm increased dynamically with the increase of anti-Dig antibody concentration; suggesting a high dependence of the affinity binding-induced Hg^{2+} releasing process on the target protein concentration. It further exhibited a linear plot between the fluorescence intensities of doped QD at 560 nm and the anti-Dig antibody concentration in the range of 0-5 nM (Figure 3B). A regression equation of Y (fluorescence intensity) = 26.6 + 399.2 X (anti-Dig antibody concentration, nM) was obtained with a correlative coefficient of about 0.9985. The detection limit toward anti-Dig antibody obtained according to the 3σ method was about 0.034 nM. This detection limit toward anti-Dig antibody was evidently lower compared with most of previously reported methods (Table S2), which might be attributed to the low background and the high responsivity of Hg^{2+} doping to QD photoluminescence for currently developed method. On the basis of six repetitive measurements toward three concentrations of anti-Dig antibody of 0.5, 1, and 10 nM, the relative standard deviation values were obtained as 4.56, 6.0, and 5.6 %, respectively, suggesting a very good detection reproducibility of the developed protein biosensor. The detection specificity toward anti-Dig antibody was further examined (Figure 3C). Almost no fluorescence responses at 560 nm of QD could be observed for the inspected non-specific

proteins. Also, the coexistence of these proteins induced no evident interference for anti-Dig antibody detection. Furthermore, the protein determination was conducted in spiked serum to investigate its applicative ability in complex biological matrix. The fluorescence intensity at 560 nm of QD also showed a linear plot with the concentration of anti-Dig antibody in the range of 0-5 nM in the serum matrix, which was almost identical with the results in the buffer (Figure 3D). The detection limit of anti-Dig antibody in the serum matrix was about 0.088 nM, which was slightly higher than that in the buffer system. Thus, the developed biosensor showed a promising prospect for use with real biological sample.

<<Herein Figure 3>>

Detection versatility of the developed protein biosensor. Since our fluorescent biosensors have modular properties, it would be readily applied for other target proteins by replacing the identified affinity ligands. In order to verify its detection versatility, two other different biosensors toward the detection of streptavidin and thrombin, respectively, were designed by simply changing the affinity ligands labeled onto the duplex AB and strand C. In the case for streptavidin detection, the biotin moiety was used as the recognition element (inset in Figure 4A). With the use of corresponding aptamers as protein recognition elements, the aptasensor could be fabricated toward the detection of thrombin as a model target protein (inset in Figure 4C).[20,26] The affinity binding of streptavidin with biotin ligands or thrombin with aptamers induces the strand displacement reaction between AB duplex and C for the Hg^{2+} releasing. The fluorescence responses after the further Hg^{2+} doping of ZnSe QD signal the analyzed protein targets. The affinity recognition-initiated strand exchange between duplex AB and C by streptavidin or thrombin was confirmed by PAGE experiments, respectively (Figure S4A and S5A). Also, the selective detection toward streptavidin or thrombin could be demonstrated, compared with other inspected proteins (Figure S4B and S5B). The detection performances toward streptavidin or thrombin were shown in Figure 4A and C, respectively. The fluorescence

signal intensity could be regulated by the streptavidin or thrombin in the concentration of 0-20 nM. The linear plots could be obtained for both streptavidin and thrombin in the concentration of 0-2 nM with the correlative coefficients of 0.9957 and 0.9964, respectively (Figure 4B and D). The detection limits for streptavidin and thrombin were determined as about 0.012 and 0.025 nM, respectively. Compared with the previously reported methods, the present biosensor exhibited a comparable or even superior detection performance toward thrombin (Table S3). It should be noted that the current strategy mainly served for the detection of proteins with multiple binding motifs, and it would be not easily applicative for the monovalent proteins. However, if the corresponding aptamer is available for the monovalent protein, a hairpin-like nucleic acid structure could be designed that contains the corresponding aptamer sequence and the incorporated Hg^{2+}. After protein interaction with its aptamer sequence, a conformation change of the nucleic acid structure might occur for Hg^{2+} releasing and succeeding QD doping-dependent fluorescence response related with protein analysis.

<<Herein Figure 4>>

CONCLUSIONS

In summary, an affinity binding-induced Hg^{2+} releasing and quantum dot doping principle was fully demonstrated for versatile, label-free, sensitive and homogenous protein quantification. The proximity recognition-initiated DNA strand exchange was committed to convey protein binding event into the released Hg^{2+}, and the succeeding Hg^{2+} doping-induced QD photoluminescence was used as a fluorogenic reporter system. The whole protein assay was operated only by a simple one-step mixing process. It presented distinctive advantages over the existing nucleic acid-based protein analysis methods, particularly in terms of label-free detection and needless of complex DNA manipulation procedures for signal readout or amplification. The detection versatility toward different proteins was verified with the detection limits of 0.034 nM (anti-Dig antibody), 0.012 nM (streptavidin) and

0.025 nM (thrombin). It hence paves a promising way for the fabrication of convenient and cost-effective biosensors by using inorganic nanocrystal doping-based signaling mechanism to serve the point-of-care applications for disease diagnosis and monitoring, biomarker screening and clinical medicine.

AUTHOR INFORMATION

Corresponding Author

* Tel. & Fax. 86-532-84022681. E-mail address: sliu@qust.edu.cn

Notes

The authors declare no competing financial interest.

Acknowledgements

We acknowledged the finance supports from the National Natural Science Foundation of China (No. 21475072), the Natural Science Foundation of Shandong Province of China (Nos. JQ201704 and ZR2015JL007), and the Key Research and Development Program of Shandong Province of China (2016GSF201208).

ASSOCIATED CONTENT

Supporting Information. The synthesized nucleic acid sequences (Table S1). The TEM image of the synthesized ZnSe QD (Figure S1). The fluorescence responses of the ZnSe QD toward different metal ions (Figure S2). The fluorescence response comparison by using motif A and C with or no Dig ligands (Figure S3). The PAGE and selectivity test toward streptavidin and thrombin (Figure S4 and 5). The detection performance comparison (Table S2 and S3). This information is available free of charge via the Internet at http://pubs.acs.org/

REFERENCES

(1) Kosaka, P. M.; Pini, V.; Ruz, J. J.; Silva, R. A. d.; González, M. U.; Ramos, D.; Calleja, M.; Tamayo, J. Detection of cancer biomarkers in serum using a hybrid mechanical and optoplasmonic nanosensor. *Nat. Nanotechnol.* **2014**, *9*, 1047-1053.

(2) Kang, D.; Sun, S.; Kurnik, M.; Morales, D.; Dahlquist, F. W.; Plaxco, K. W. New architecture for reagentless, protein-based electrochemical biosensors. *J. Am. Chem. Soc.* **2017**, *139*, 12113-12116.

(3) Labib, M.; Sargent, E. H.; Kelley, S. O. Electrochemical methods for the analysis of clinically relevant biomolecules. *Chem. Rev.* **2016**, *116*, 9001-9090.

(4) Huang, X.; Liu, Y.; Yung, B.; Xiong, Y.; Chen, X. Nanotechnology-enhanced no-wash biosensors for *in vitro* diagnostics of cancer. *ACS Nano* **2017**, *11*, 5238-5292.

(5) Han, X. X.; Jia, H. Y.; Wang, Y. F.; Lu, Z. C.; Wang, C. X.; Xu, W. Q.; Zhao, B.; Ozaki, Y. Analytical technique for label-free multi-protein detection based on western blot and surface-enhanced raman scattering. *Anal. Chem.* **2008**, *80*, 2799-2804.

(6) Bakalova, R.; Zhelev, Z.; Ohba, H.; Baba, Y. Quantum dot-based western blot technology for ultrasensitive detection of tracer proteins. *J. Am. Chem. Soc.* **2005**, *127*, 9328-9329.

(7) Lai, S.; Wang, S.; Luo, J.; Lee, L. J.; Yang, S. T.; Madou, M. J. Design of a compact disk-like microfluidic platform for enzyme-linked immunosorbent assay. *Anal. Chem.* **2004**, *76*, 1832-1837.

(8) Yang, Z. H.; Zhuo, Y.; Yuan, R.; Chai, Y. Q. Highly effective protein converting strategy for ultrasensitive electrochemical assay of cystatin C. *Anal. Chem.* **2016**, *88*, 5189-5196.

(9) Li, F.; Zhang, H.; Lai, C.; Li, X. F.; Le, X. C. A molecular translator that acts by binding-induced DNA strand displacement for a homogeneous protein assay. *Angew. Chem., Int. Ed.* **2012**, *51*, 9317-9320.

(10) Zhang, L.; Zhang, K.; Liu, G.; Liu, M.; Liu, Y.; Li, J. Label-free nanopore proximity bioassay for platelet-derived growth factor detection. *Anal. Chem.*

2015, *87*, 5677-5682.

(11) Ranallo, S.; Rossetti, M.; Plaxco, K. W.; Vallée-Bélisle, A.; Ricci, F. A modular, DNA-based beacon for single-step fluorescence detection of antibodies and other proteins. *Angew.Chem., Int. Ed.* **2015**, *54*, 13214-13218.

(12) Porchetta, A.; Ippodrino, R.; Marini, B.; Caruso, A.; Caccuri, F.; Ricci, F. Programmable nucleic acid nanoswitches for the rapid, single-step detection of antibodies in bodily fluids. *J. Am. Chem. Soc.* **2018**, *140*, 947-953.

(13) Wu, Z.; Zhen, Z.; Jiang, J. H.; Shen, G. L.; Yu, R. Q. Terminal protection of small-molecule-linked DNA for sensitive electrochemical detection of protein binding via selective carbon nanotube assembly. *J. Am. Chem. Soc.* **2009**, *131*, 12325-12332.

(14) Cao, Y.; Zhu, S.; Yu, J.; Zhu, X.; Yin, Y.; Li, G. Protein detection based on small molecule-linked DNA. *Anal. Chem.* **2012**, *84*, 4314-4320.

(15) Liu, S.; Cheng, C.; Gong, H.; Wang, L. Programmable Mg^{2+}-dependent DNAzyme switch by the catalytic hairpin DNA assembly for dual-signal amplification toward homogeneous analysis of protein and DNA. *Chem. Commun.* 2015, 51, 7364-7367.

(16) Hu, J.; Yu, Y.; Brooks, J. C.; Godwin, L. A.; Somasundaram, S.; Torabinejad, F.; Kim, J.; Shannon, C.; Easley, C. J. A reusable electrochemical proximity assay for highly selective, real-time protein quantitation in biological matrices. *J. Am. Chem. Soc.* **2014**, *136*, 8467-8474.

(17) Zhang, Y. L.; Huang, Y.; Jiang, J. H.; Shen, G. L.; Yu, R. Q. Electrochemical aptasensor based on proximity-dependent surface hybridization assay for single-step, reusable, sensitive protein detection. *J. Am. Chem. Soc.* **2007**, *129*, 15448-15449.

(18) Fredriksson, S.; Gullberg, M.; Jarvius, J.; Olsson, C.; Pietras, K.; Gústafsdóttir, S. M.; Ostman, A.; Landegren, U. Protein detection using proximity-dependent DNA ligation assays. *Nat. Biotechnol.* **2002**, *20*, 473-477.

(19) Chen, J.; Deng, B.; Wu, P.; Li, F.; Li, X. F.; Le, X. C.; Zhang, H.; Hou, X. Amplified binding-induced homogeneous assay through catalytic cycling of analyte for ultrasensitive protein detection. *Chem. Commun.* **2016**, *52*,

1816-1819.

(20) Li, J.; Zhong, X.; Zhang, H.; Le, X. C.; Zhu, J. J. Binding-induced fluorescence turn-on assay using aptamer-functionalized silver nanocluster DNA probes. *Anal. Chem.* **2012**, *84*, 5170-5174.

(21) Tang, Y.; Lin, Y.; Yang, X.; Wang, Z.; Le, X. C.; Li, F. Universal strategy to engineer catalytic DNA hairpin assemblies for protein analysis. *Anal. Chem.* **2015**, *87*, 8063-8066.

(22) Ranallo, S.; Prévost-Tremblay, C.; Idili, A.; Vallée-Bélisle, A.; Ricci, F. Antibody-powered nucleic acid release using a DNA-based nanomachine. *Nat. Commun.* **2017**, *8*, 15150.

(23) Chen, J.; Zuehlke, A.; Deng, B.; Peng, H.; Hou, X.; Zhang, H. A target-triggered DNAzyme motor enabling homogeneous, amplified detection of proteins. *Anal. Chem.* **2017**, *89*, 12888-12895.

(24) Wei, L.; Wang, X.; Wu, D.; Li, C.; Yin, Y.; Li, G. Proximity ligation-induced assembly of DNAzymes for simple and cost-effective colourimetric detection of proteins with high sensitivity. *Chem. Commun.* **2016**, *52*, 5633-5636.

(25) Zhang, H.; Li, F.; Dever, B.; Wang, C.; Li, X. F.; Le, X. C. Assembling DNA through affinity binding to achieve ultrasensitive protein detection. *Angew. Chem., Int. Ed.* **2013**, *52*, 10698-10705.

(26) Yang, J.; Dou, B.; Yuan, R.; Xiang, Y. Proximity binding and metal ion-dependent DNAzyme cyclic amplification-integrated aptasensor for label-free and sensitive electrochemical detection of thrombin. *Anal. Chem.* **2016**, *88*, 8218-8223.

(27) Bertucci, A.; Porchetta, A.; Ricci, F. Antibody-templated assembly of an RNA mimic of green fluorescent protein. *Anal. Chem.* **2018**, *90*, 1049-1053.

(28) Guo, B.; Sheng, Y.; Zhou, K.; Liu, Q.; Liu, L.; Wu, H. C. Analyte-triggered DNA-probe release from a triplex molecular beacon for nanopore sensing. *Angew. Chem., Int. Ed.* **2018**, *57*, 3602-3606.

(29) Tian, Y.; Zhang, S.; Wang, L.; Liu, S. A modular nanoswitch for mix-and-detect protein assay based on binding-induced cascade dissociation

of kissing complex. *ChemBioChem* **2018**, *19*, 716-722.

(30) Hu, X.; Li, C.; Feng, C.; Mao, X.; Xiang, Y.; Li, G. One-step colorimetric detection of an antibody based on protein-induced unfolding of a G-quadruplex switch. *Chem. Commun.* **2017**, *53*, 4692-4694.

(31) Zhang, Z.; Hejesen, C.; Kjelstrup, M. B.; Birkedal, V.; Gothelf, K. V. A DNA-mediated homogeneous binding assay for proteins and small molecules. *J. Am. Chem. Soc.* **2014**, *136*, 11115-11120.

(32) Mahshid, S. S.; Ricci, F.; Kelley, S. O.; Vallée-Bélisle, A. Electrochemical DNA-based immunoassay that employs steric hindrance to detect small molecules directly in whole blood. *ACS Sens.* **2017**, *2*, 718-723

(33) Miyake, Y.; Togashi, H.; Tashiro, M.; Yamaguchi, H.; Oda, S.; Kudo, M.; Tanaka, Y.; Kondo, Y.; Sawa, R.; Fujimoto, T.; Machinami, T.; Ono, A. Mercury^{II}-mediated formation of thymine-Hg^{II}-thymine base pairs in DNA duplexes. *J. Am. Chem. Soc.* **2006**, *128*, 2172-2173.

(34) Tanaka, Y.; Oda, S.; Yamaguchi, H.; Kondo, Y.; Kojima, C.; Ono, A. ^{15}N-^{15}N *J*-coupling across Hg^{II}: direct observation of Hg^{II}-mediated T-T base pairs in a DNA duplex. *J. Am. Chem. Soc.* **2007**, *129*, 244-245.

(35) Xue, X.; Wang, F.; Liu, X. One-step, room temperature, colorimetric detection of mercury (Hg^{2+}) using DNA/nanoparticle conjugates. *J. Am. Chem. Soc.* **2008**, *130*, 3244–3245.

(36) Clever, G. H.; Kaul, C.; Carell, T. DNA-metal base pairs. *Angew. Chem., Int. Ed.* **2007**, *46*, 6226- 6236.

(37) Pradhan, N.; Goorskey, D.; Thessing, J.; Peng, X. An alternative of CdSe nanocrystal emitters: pure and tunable impurity emissions in ZnSe nanocrystals. *J. Am. Chem. Soc.* **2005**, *127*, 17586-17587.

(38) Wu, P.; Yan, X. P. Doped quantum dots for chemo/biosensing and bioimaging. *Chem. Soc. Rev.* **2013**, *42*, 5489-5521.

(39) Zhou, Z. Q.; Yang, L. Y.; Yan, R.; Zhao, J.; Liu, Y. Q.; Lai, L.; Jiang, F. L.; Maskow, T.; Liu, Y. Mn-doped ZnSe quantum dots initiated mild and rapid cation exchange for tailoring the composition and optical properties of colloid nanocrystals: novel template, new applications. *Nanoscale* **2017**, *9*, 2824-2835.

(40) Li, F.; Zhang, H.; Wang, Z.; Li, X.; Li, X. F.; Le, X. C. Dynamic DNA assemblies mediated by binding-induced DNA strand displacement. *J. Am. Chem. Soc.* **2013**, *135*, 2443-2446.

(41) Li, F.; Tang, Y.; Traynor, S. M.; Li, X. F.; Le, X. C. Kinetics of proximity-induced intramolecular DNA strand displacement. *Anal. Chem.* **2016**, *88*, 8152-8157.

(42) Gill, R.; Zayats, M.; Willner, I. Semiconductor quantum dots for bioanalysis. *Angew. Chem., Int. Ed.* **2008**, *47*, 7602-7625.

(43) Silvi, S.; Credi, A. Luminescent sensors based on quantum dot-molecule conjugates. *Chem. Soc. Rev.* **2015**, *44*, 4275-4289.

(44) Zhou, J.; Yang, Y.; Zhang, C. Y. Toward biocompatible semiconductor quantum dots: from biosynthesis and bioconjugation to biomedical application. *Chem. Rev.* **2015**, *115*, 11669-11717.

(45) He, X.; Ma, N. A general strategy for label-free sensitive DNA detection based on quantum dot doping. *Anal. Chem.* **2014**, *86*, 3676-3681.

Figure Captions

Scheme 1. Schematic illustration of the fabricated protein biosensor by affinity binding-induced Hg^{2+} releasing and doping-induced QD photoluminescence.

Figure 1. (A) TEM images of synthesized ZnSe QD. (B) XPS spectra of ZnSe QD (black line) and doped ZnSe QD with excess Hg^{2+} (red line). (C) Fluorescence spectra of ZnSe QD after mixing with various concentrations of Hg^{2+} ions. The Hg^{2+} concentrations from curves a to j were 0, 0.5 nM, 1 nM, 2 nM, 4 nM, 6 nM, 10 nM, 15 nM, 20 nM, 50 nM, respectively. (D) Relationship of fluorescence intensity of ZnSe QD at 560 nm with the added Hg^{2+} concentration. The obtained error bars were based on three repetitive experimental results.

Figure 2. (A) Relative absorbance, $A = (A_{t\,℃} - A_{10\,℃})/(A_{90\,℃} - A_{10\,℃})$ at 260 nm versus temperature for a mixture of motif A and strand B with (red line) or no (black line) addition of 2 μM Hg^{2+}. Each solution contained 1 μM motif A and strand B in Tris buffer (0.05 M, pH 7.5). (B) Fluorescence spectra for the ZnSe QD (black line), doped QD with 20 nM Hg^{2+} (green line), and the incubation of ZnSe QD with 10 nM duplex AB and 10 nM motif C in the absence (red line) and presence of 10 nM anti-Dig antibody (blue line). (C) Native PAGE characterization toward protein recognition-initiated DNA strand exchange reaction: lane 1, a mixture containing 2 μM duplex AB, 2 μM motif C, and 1 μM anti-Dig antibody; lane 2, 2 μM duplex AB and 2 μM motif C; lane 3, 2 μM motif C; lane 4, 2 μM duplex AB; lane 5, low molecular DNA ladder. (D) Fluorescence intensities of QD at 560 nm as a function of incubation time for the mixture of 10 nM duplex AB, 10 nM motif C and 10 nM anti-Dig antibody. The obtained error bars were based on three repetitive experimental results.

Figure 3. (A) Fluorescence spectra of QD titrated with various concentrations of anti-Dig antibody: a) 0, b) 0.2, c) 0.5, d) 1, e) 2, f) 5, g) 10, h) 15, i) 20 nM, respectively. (B) Relationship of fluorescence intensities at 560 nm of QD with anti-Dig antibody concentrations. Inset shows the linear plot. (C) Selectivity

test of the fabricated protein biosensor for anti-Dig antibody against different proteins: 1) blank, 2) BSA, 3) AFP, 4) IgG, 5) thrombin, 6) streptavidin, 7) anti-Dig antibody, 8) anti-Dig antibody and thrombin, 9) anti-Dig antibody and streptavidin, 10) anti-Dig antibody and IgG, 11) the mixture of anti-Dig antibody, thrombin, streptavidin and IgG. Each tested protein has a concentration of 10 nM. (D) Relationship of fluorescence intensities at 560 nm of QD with anti-Dig antibody concentration spiked in diluted serum (1: 10). Inset shows the corresponding fluorescence spectra at various anti-Dig antibody concentrations: a) 0, b) 0.2, c) 0.5, d) 1, e) 2, f) 5, g) 10 nM, respectively. Error bars in B-D were obtained based on three repetitive experimental results.

Figure 4. (A) Fluorescence spectra obtained at various concentrations of streptavidin. The streptavidin concentrations for the curves (a) to (i) are: 0, 0.05, 0.2, 0.5, 1, 2, 5, 10, 20 nM, respectively. (B) The calibration curve between the fluorescence intensity and the streptavidin concentration. The linear plot between them is shown in Inset. (C) The fluorescence spectra obtained at various thrombin concentrations. The thrombin concentrations for the curves (a) to (i) are: 0, 0.1, 0.2, 0.5, 1, 2, 5, 10, 20 nM, respectively. (D) The calibration curve between the fluorescence intensity and the thrombin concentration. Inset shows the linear plot. The inset in Figure 4A and C illustrates the schematic diagram for streptavidin and thrombin detection, respectively.

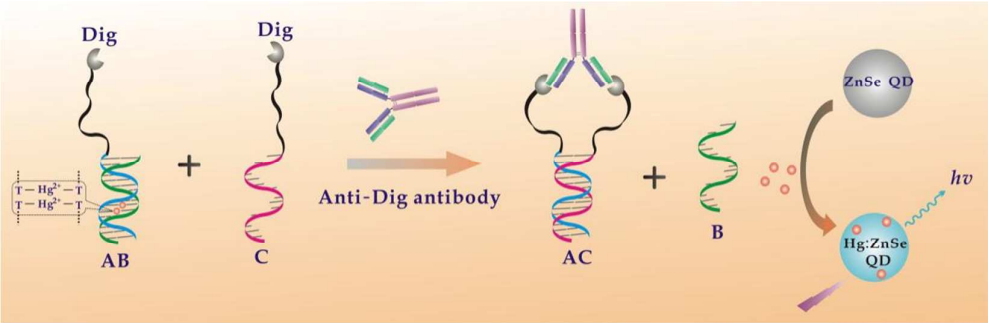
Dig
Dig
T — Hg2+ — T
T — Hg2+ — T
AB
C
Anti-Dig antibody
AC
B
ZnSe QD
Hg:ZnSe QD
hv

Scheme 1

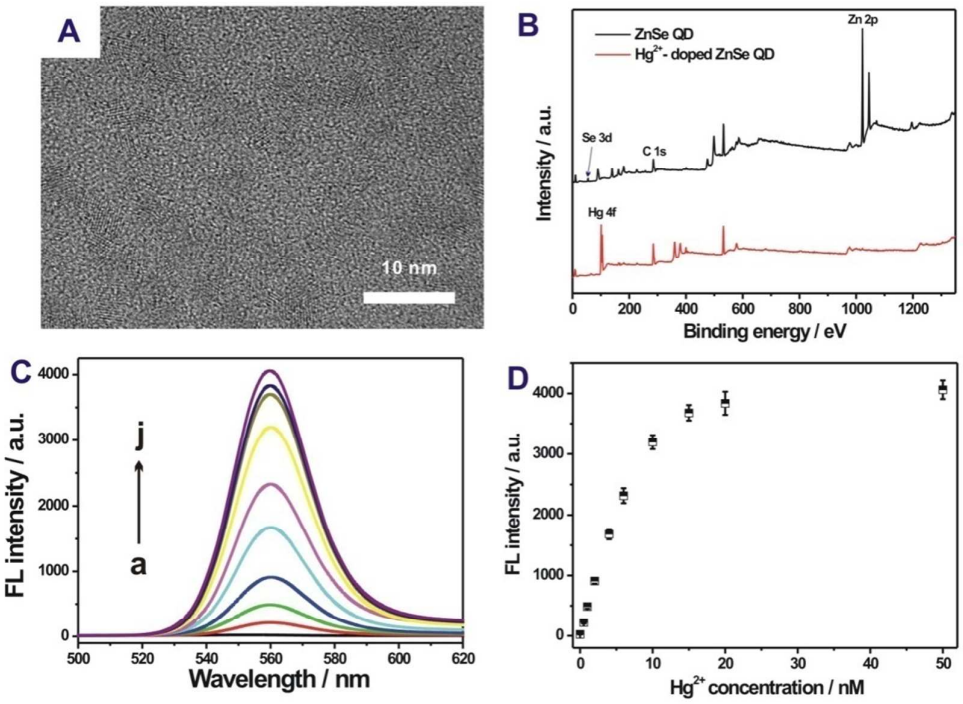
A
10 nm
B
ZnSe QD
Hg2+- doped ZnSe QD
Zn 2p
Se 3d
C 1s
Hg 4f
Intensity / a.u.
Binding energy / eV
C
j
a
FL intensity / a.u.
Wavelength / nm
D
FL intensity / a.u.
Hg2+ concentration / nM

Figure 1

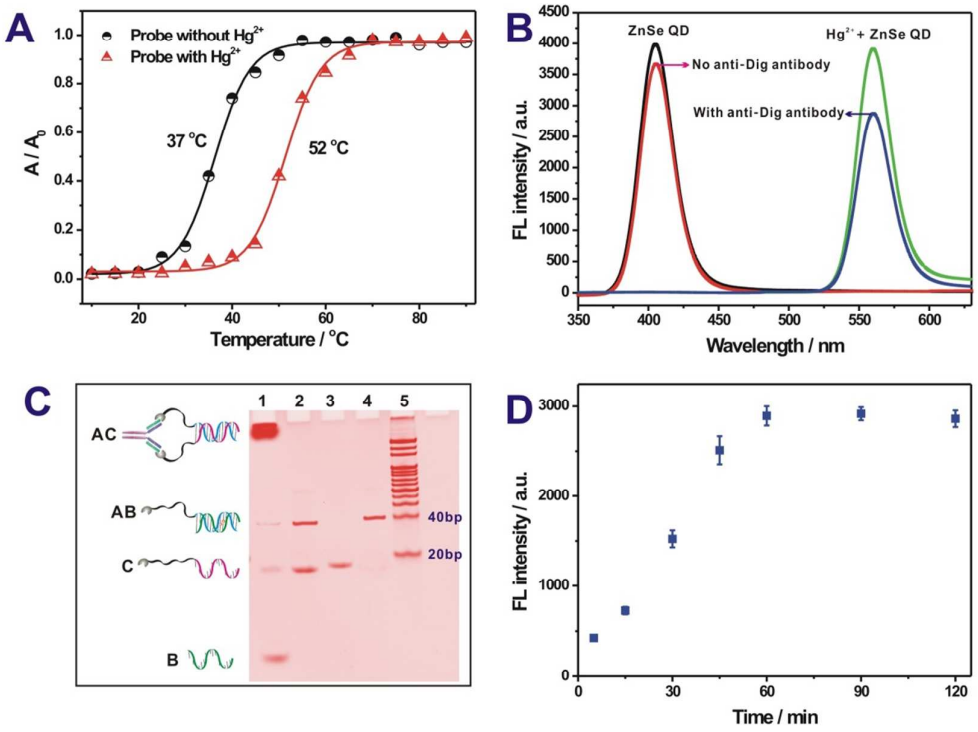
A
Probe without Hg2+
Probe with Hg2+
37 °C
52 °C
A / A0
Temperature / °C
B
ZnSe QD
Hg2+ + ZnSe QD
No anti-Dig antibody
With anti-Dig antibody
FL intensity / a.u.
Wavelength / nm
C
1 2 3 4 5
AC
AB
C
B
40bp
20bp
D
FL intensity / a.u.
Time / min

Figure 2

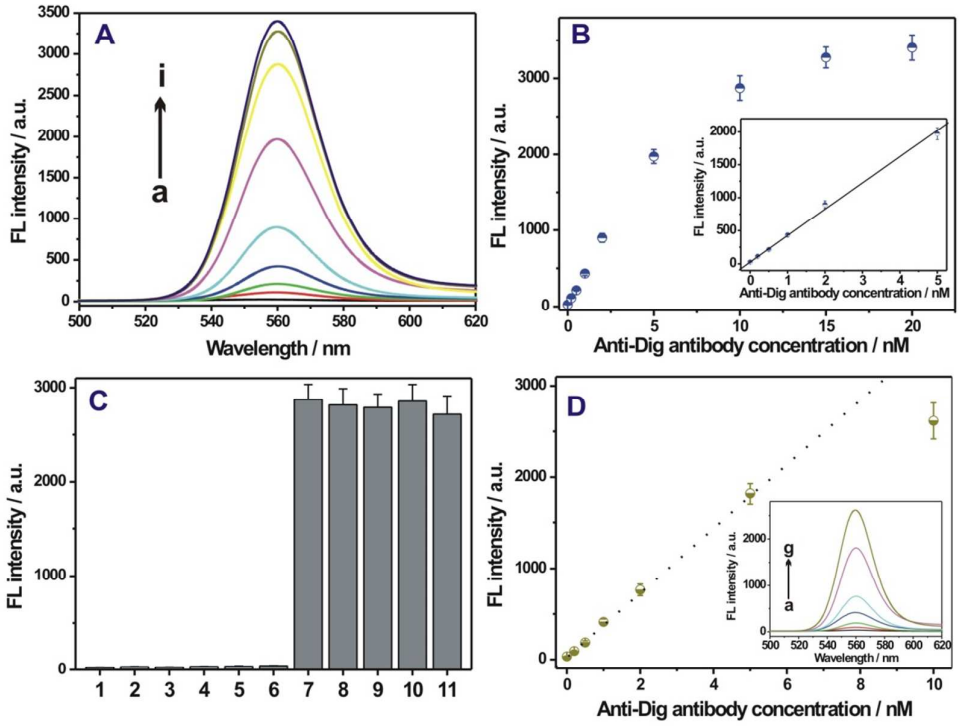
A
i
a
FL intensity / a.u.
Wavelength / nm
B
FL intensity / a.u.
Anti-Dig antibody concentration / nM
C
FL intensity / a.u.
D
FL intensity / a.u.
Anti-Dig antibody concentration / nM
g
a
Wavelength / nm

Figure 3

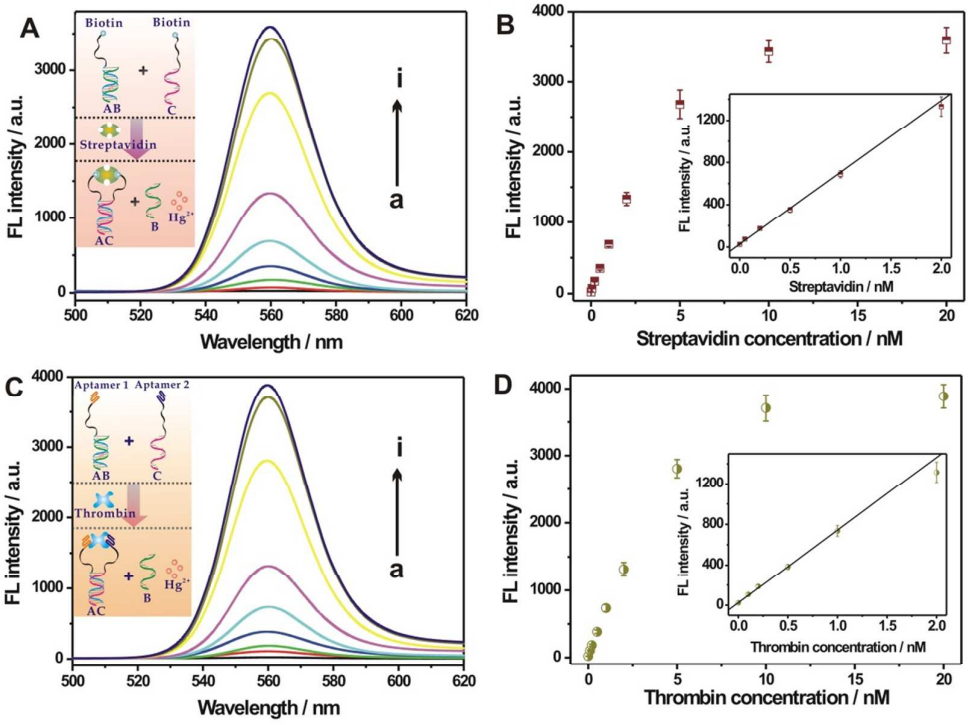
A
Biotin
Biotin
AB
C
Streptavidin
AC
B
Hg2+
FL intensity / a.u.
Wavelength / nm
i
a
B
FL intensity / a.u.
Streptavidin concentration / nM
Streptavidin / nM
C
Aptamer 1
Aptamer 2
Thrombin
D
Thrombin concentration / nM

Figure 4

For TOC only